

# Gradient Flow Structure and Quantitative Dynamics of Multi-Head Self-Attention

Ayan Pendharkar

May 2026

## Abstract

Transformer self-attention can be viewed as a gradient flow on the unit sphere, where tokens evolve under softmax interaction potentials and collapse into clusters. Prior work establishes clustering for single-head flows. The multi-head setting is more complex, as heads interfere with each other geometrically, and the single-head monotonicity argument breaks down.

We build a framework for the multi-head dynamics and resolve several open questions. Under explicit conditions on the score matrices, we prove the total energy  $\mathcal{E}_{\text{multi}}$  is non-decreasing along both flat and sphere dynamics (Theorem 11). For individual heads, we identify the exact obstruction: radial shadows, projections of each head's output onto the token position, that survive even when the head subspaces are exactly orthogonal. We give a sufficient condition (Radial Dominance, Condition 8) and a robustness result for approximate orthogonality (Theorem 39). In the scalar-head, equiangular-token regime (Section 2.3), we derive the critical inverse temperature  $\beta^*$  in closed form via the golden ratio and the Lambert  $W$ -function (Theorem 19), and prove super-additivity of clustering rates for heterogeneous heads (Theorem 22). Under the same assumptions, we prove an  $O(n \log d)$  vs.  $O(n)$  clustering-time separation between ReLU and softmax attention in the linearized regime near  $\gamma = 0$  (Theorem 25). Finally, we establish an exact entropy production identity (Theorem 27) and prove, in the scalar-head equiangular case, that attention entropy is monotonically non-decreasing: it increases toward  $\log n$  as tokens cluster and attention equalizes, then stabilizes as the dynamics halt.

## 1 Introduction

### Background

Since Geshkovski, Letrouit, Polyanskiy, and Rigollet [9, 10] first modeled transformer tokens as particles on the unit sphere evolving under softmax interactions, the clustering behavior of self-attention has become a central object of study. In their framework,  $n$  layer-normalized tokens on  $S^{d-1}$  follow a gradient flow, and the key result is collapse to a common point or a small number of clusters in finite time. This is analogous to synchronization in coupled oscillator models [14], and is widely believed to be the mechanism behind the semantic compression that makes transformers effective. Quantitative control over clustering has direct consequences for training stability [21] and long-context behavior [5]. The synchronization perspective is developed further in [7] for sphere dynamics with nonlinear interactions and in [15] on the circle.

### The multi-head gap

Every rigorous result in this line of work concerns single-head attention. Real transformers use  $H$  heads in parallel, each with its own score matrix  $M_h \in \mathbb{R}^{d \times d}$ . The token velocity is a sum of per-head contributions, and this creates a geometric problem that the existing theory does not address.

The issue is not obvious at first. If the heads operate on orthogonal subspaces ( $M_{h'}M_h = 0$  for  $h' \neq h$ ), one might expect cross-head interference to vanish. It does not. The projection of each head’s output onto the token’s current position, which we call a *radial shadow*, is not killed by subspace orthogonality. These shadows create coupling terms in the per-head energy derivative that have no analogue in the single-head case.

To see why concretely: on the sphere, the velocity  $\dot{x}_i = \frac{1}{n} \sum_h f_i^h$  gets projected tangentially via  $P_{x_i}^\perp(\cdot)$ . This projection mixes contributions from all heads in a way that blocks the naive extension of the single-head monotonicity argument.

## This paper

We build a rigorous framework for multi-head gradient flow dynamics and resolve several of these open questions. The main contributions are as follows.

**(i) Total energy monotonicity (Theorem 11).** Under score symmetry (Condition 3) and value alignment (Condition 4), the total energy  $\mathcal{E}_{\text{multi}} = \sum_h \mathcal{E}^h$  is non-decreasing along both flat and sphere dynamics:

$$\frac{d\mathcal{E}_{\text{multi}}}{dt} = \frac{1}{n} \sum_{i=1}^n \|\dot{x}_i\|^2 \geq 0.$$

**(ii) Per-head monotonicity and the radial shadow obstruction (Theorems 16–17).** In flat space, per-head monotonicity follows from subspace orthogonality alone (Condition 6). On the sphere it does not. The residual cross-head radial shadow  $\sum_{h' \neq h} a_i^{h'}$ , where  $a_i^{h'} = \langle f_i^{h'}, x_i \rangle$ , persists even under exact orthogonality. We give the sufficient condition (Condition 8, Radial Dominance) under which it is controlled. Theorem 39 then shows the result is robust to approximate orthogonality  $\|M_{h'}M_h\|_{\text{op}} \leq \delta$ , which is the practically relevant case since trained transformers have principal angles of 70–85°, not 90°.

**(iii) Critical temperature (Theorem 19).** In the scalar-head, orthogonal-token regime: for  $M_h = \alpha I$  and mutually orthogonal tokens, Condition 8 holds if and only if  $\beta \leq \beta^*$ , where

$$\beta^* = \frac{1}{2\alpha} \ln \frac{c^*(H)^2(n-1)}{1 - c^*(H)^2}, \quad c^*(H) = \frac{\sqrt{(H-1)^2 + 4} - (H-1)}{2}.$$

For  $H = 2$ , the threshold is  $c^*(2) = (\sqrt{5} - 1)/2 = 1/\varphi$ , the reciprocal of the golden ratio. For general  $H$ , it can be expressed via the Lambert  $W$ -function.

**(iv) Heterogeneous convergence and super-additivity (Theorem 22).** In the scalar-head, equiangular-token regime: for heads with distinct strengths  $\lambda_h$ , the late-time clustering rate is  $\varepsilon(t) \sim Ce^{-2\Lambda t}$  where  $\Lambda = \sum_h \lambda_h$ . The early-time rate per head is  $g^h(0) = 2\lambda_h/(e^{\lambda_h\beta} + n - 1)$ , maximized at  $\lambda^*\beta = 1 + W((n-1)/e)$ . When the mean head strength  $\bar{\lambda}$  exceeds the inflection point  $\lambda_c$  of the rate function, spreading the head strengths strictly increases the early-time clustering rate over  $H$  equal heads at the same total budget. This is a super-additivity result suggesting that head diversity is geometrically beneficial.

**(v) ReLU vs. softmax clustering time (Theorem 25).** In the scalar-head, equiangular-token, linearized regime: for random tokens on  $S^{d-1}$  with  $\gamma_0 = O(1/\sqrt{d})$ ,

$$T_{\text{ReLU}} = O(n \log d) \quad \text{vs.} \quad T_{\text{softmax}} = O(n).$$

The reason is simple:  $\text{ReLU}(0) = 0$ , so ReLU attention has zero driving force at  $\gamma = 0$ , while softmax has a positive constant  $c_0 = 2\lambda/(e^{\lambda\beta} + n - 1)$  regardless of dimension. A full proof for the nonlinear regime is deferred to Open Problem 5.

(vi) **Entropy production identity (Theorem 27).** We prove the exact identity

$$\frac{dH_i^h}{dt} = -\beta^2 \text{Cov}_{p_i^h}(s_j, \dot{s}_j),$$

and show, in the scalar-head equiangular case, that  $\text{Cov}_p(s_j, \dot{s}_j) \leq 0$ , so entropy is non-decreasing (Corollary 30). During pre-clustering,  $|\text{Cov}(s_j, \dot{s}_j)| \gg 0$  and entropy rises quickly as scores equalize and attention spreads toward uniform. Near full clustering, score velocities  $\dot{s}_j \rightarrow 0$  and entropy stabilizes at  $\log n$ .

## What is new

The single-head theory of [9, 10] is the direct predecessor of this work. The contributions that are absent from the prior literature are as follows.

- **Coupled multi-head gradient flow formulation.** The first rigorous treatment of the  $H$ -head flow as a single dynamical system, showing the combined velocity field  $\frac{1}{n} \sum_h f_i^h$  is the gradient of  $\mathcal{E}_{\text{multi}}$  (Theorem 11).
- **Radial shadow obstruction.** Even under exact orthogonality ( $M_{h'} M_h = 0$ ), per-head monotonicity fails on the sphere because the radial projections  $\langle f_i^{h'}, x_i \rangle$  survive. This cross-head interference has no single-head analogue.
- **Radial Dominance condition and critical temperature.** The first sufficient condition (Condition 8) under which per-head energy monotonicity holds on the sphere, with its exact threshold  $\beta^*$  computed in closed form for scalar heads.
- **Quantitative rates for heterogeneous heads.** In the scalar-equiangular regime, Theorem 22 establishes super-additivity of early-time clustering rates when head strengths enter the convex regime of the rate function.
- **Exact entropy production identity.** Theorem 27 provides the identity  $dH_i^h/dt = -\beta^2 \text{Cov}_p(s_j, \dot{s}_j)$ , valid for any score-symmetric attention with sphere dynamics, making the direction of entropy change computable.

## Relation to prior work

Our setup follows Geshkovski et al. [9, 10] and Rigollet [16]. The single-head clustering result of [10], based on a cone-collapse argument, does not extend to the combined velocity field  $\sum_h f_i^h$ ; whether all stable critical points of the multi-head flow are complete clusters remains open (Open Problem 2). We treat the normalized flow of Karagodin et al. [12] in Theorem 21 and show the log-partition energy  $G = \frac{1}{\beta n} \sum_i \log Z_i$  does not inherit monotonicity, complementing their analysis. The quantitative rates of [4] complement our per-head convergence analysis (Theorem 40); Theorem 22 extends their analysis to the multi-head case. Tomihari and Karakida [18] analyze recurrent self-attention from a Jacobian perspective without a Lyapunov function; our energy-based approach is complementary. The entropy identity (Theorem 27) complements the entropy-collapse analysis of Zhai et al. [21] with an exact differential relation along the flow, and connects to the entropy-guided attention of Jha and Reagen [11]. We consider unmasked attention throughout; the causal setting is analyzed in [13].

## Organization

Section 2 sets up notation, the token dynamics on  $S^{d-1}$ , and the two projection identities used throughout. It also contains the Standing Assumptions table (Section 2.4) listing exactly which conditions each result requires. Section 3 proves total energy monotonicity. Section 4

handles per-head monotonicity and identifies the radial shadow obstruction. Section 5 derives  $\beta^*$  in closed form. Section 6 treats the normalized flow. Sections 7–11 develop the quantitative results. Section 12 summarizes and identifies the main open directions. Section 13 states open problems.

## 2 Setup and Notation

### 2.1 Tokens, Energy, and Dynamics

Let  $x_1, \dots, x_n \in S^{d-1} = \{v \in \mathbb{R}^d : \|v\| = 1\}$  be  $n$  tokens on the unit sphere. This models layer-normalized [2] transformer representations, since dividing by the norm after each layer is exactly projection onto  $S^{d-1}$ .

For each head  $h \in \{1, \dots, H\}$ , let  $M_h \in \mathbb{R}^{d \times d}$  be the score matrix (encoding the combined query and key projections) and  $\beta > 0$  the inverse temperature. The **per-head interaction energy** is

$$\mathcal{E}^h(X) = \frac{1}{2\beta n^2} \sum_{i=1}^n \sum_{j=1}^n e^{\beta \langle x_i, M_h x_j \rangle}. \quad (1)$$

The prefactor  $1/(2\beta n^2)$  is chosen so the derivative has a clean form: the  $\beta$  from differentiating  $e^{\beta \langle \cdot \rangle}$  cancels with  $1/\beta$ , and  $n^2$  accounts for the number of pairs. The **total multi-head energy** is  $\mathcal{E}_{\text{multi}} = \sum_{h=1}^H \mathcal{E}^h$ .

For head  $h$  and token  $i$ , the **attention-weighted aggregation** is

$$f_i^h = \sum_{j=1}^n e^{\beta \langle x_i, M_h x_j \rangle} M_h x_j. \quad (2)$$

The **multi-head velocity** at token  $i$  is

$$v_i = \frac{1}{n} \sum_h f_i^h. \quad (3)$$

Since tokens live on  $S^{d-1}$ , motion must be tangential. The **tangential projection** at  $x \in S^{d-1}$  is

$$P_x^\perp(v) = v - \langle v, x \rangle x, \quad (4)$$

which removes the radially outward component of  $v$ . The **sphere dynamics** are  $\dot{x}_i = P_{x_i}^\perp(v_i)$ .

### 2.2 Two Fundamental Projection Identities

These two identities appear in every proof that follows.

**Identity 1** (K — Self-pairing). For any  $x \in S^{d-1}$  and  $u \in \mathbb{R}^d$ ,

$$\langle P_x^\perp(u), u \rangle = \|P_x^\perp(u)\|^2.$$

*Proof.* Expand the left side using  $P_x^\perp(u) = u - \langle u, x \rangle x$ :

$$\langle u - \langle u, x \rangle x, u \rangle = \|u\|^2 - \langle u, x \rangle^2.$$

Expand the right side:

$$\|u - \langle u, x \rangle x\|^2 = \|u\|^2 - 2\langle u, x \rangle^2 + \underbrace{\langle u, x \rangle^2 \|x\|^2}_{=1} = \|u\|^2 - \langle u, x \rangle^2.$$

Both sides are equal. □

**Identity 2** (SA — Symmetry of  $P_x^\perp$ ). For any  $x \in S^{d-1}$  and  $u, w \in \mathbb{R}^d$ ,

$$\langle P_x^\perp(u), w \rangle = \langle u, P_x^\perp(w) \rangle.$$

*Proof.*

$$\langle P_x^\perp(u), w \rangle = \langle u - \langle u, x \rangle x, w \rangle = \langle u, w \rangle - \langle u, x \rangle \langle x, w \rangle.$$

$$\langle u, P_x^\perp(w) \rangle = \langle u, w - \langle w, x \rangle x \rangle = \langle u, w \rangle - \langle w, x \rangle \langle u, x \rangle.$$

The two expressions are equal since  $\langle u, x \rangle \langle x, w \rangle = \langle w, x \rangle \langle u, x \rangle$ .  $\square$

## 2.3 Conditions on Score Matrices

The following conditions are imposed on the score matrices. Not every theorem needs all of them; the exact requirements are stated with each result and summarized in the Standing Assumptions table (Section 2.4).

**Condition 3** (S — Score Symmetry).  $M_h = M_h^\top$  for all  $h$ . This makes the kernel  $e^{\beta \langle x_i, M_h x_j \rangle}$  symmetric in  $(i, j)$  and enables index-swap arguments in the proofs.

**Condition 4** (V — Value Alignment). The value projection satisfies  $W^{V,h} = M_h$  for all  $h$ . This identifies the aggregation (2) with the energy gradient, making the velocity  $v_i = \frac{1}{n} \sum_h f_i^h$  consistent with the chain rule applied to  $\mathcal{E}_{\text{multi}}$ .

*Remark 5* (Scope of Condition 4). Setting  $W^{V,h} = M_h$  ties the value projection to the score matrix, which is not the case in general transformers where query/key and value projections are independent. This is the main idealization of our framework. In practice,  $W^{V,h} = M_h + E_h$  for some perturbation  $E_h$ , and Theorem 12 shows that total energy monotonicity survives small  $\|E_h\|_{\text{op}}$ , paralleling the robustness result of Theorem 39.

**Condition 6** (O — Orthogonal Subspaces).  $M_{h'} M_h = 0$  for all  $h' \neq h$ . Since  $f_i^h \in \text{Im}(M_h)$ , this forces  $M_{h'} f_i^h = 0$ , killing operator-level cross-head terms.

**Condition 7** (P — Projection Structure).  $M_h^2 = M_h$  for all  $h$ , so each  $M_h$  is an orthogonal projection. Combined with Condition 3, this means  $M_h$  projects onto its column space. In particular,  $M_h$  acts as the identity on  $\text{Im}(M_h)$ : if  $u \in \text{Im}(M_h)$ , then  $M_h u = u$ .

**Condition 8** ( $\tau$  — Radial Dominance). For each head  $h$  and token  $i$ ,

$$\sum_{h' \neq h} |a_i^{h'}| \leq \frac{(b_i^h)^2}{\|f_i^h\|},$$

where  $a_i^h, b_i^h$  are defined in Definition 10 below. This controls the residual radial shadows on the sphere.

*Remark 9* (Naming convention). Condition 8 governs per-head energy monotonicity on the sphere and appears in Sections 4–5. A separate entropy condition, **Condition E**, appears later in Proposition 34 and is unrelated. The different labels ( $\tau$  vs. E) are intentional.

**Definition 10** (Radial-tangential decomposition). For each head  $h$  and token  $i$ , define:

- the **radial component**  $a_i^h = \langle f_i^h, x_i \rangle$  (projection of head  $h$ 's aggregation onto the token position),
- the **tangential magnitude**  $b_i^h = \|P_{x_i}^\perp(f_i^h)\| = \|f_i^h - a_i^h x_i\|$ ,
- the **alignment fraction**  $\rho_i^h = |a_i^h| / \|f_i^h\| = |\cos \theta_i^h|$ , where  $\theta_i^h$  is the angle between  $f_i^h$  and  $x_i$ .

By Pythagoras:  $(a_i^h)^2 + (b_i^h)^2 = \|f_i^h\|^2$ .

**Degenerate case.** If  $\|f_i^h\| = 0$ , then  $a_i^h = b_i^h = \rho_i^h = 0$ . For generic initial data on  $S^{d-1}$  with  $d \geq 2$ ,  $\|f_i^h\| > 0$  for all  $i, h$ . Indeed,  $f_i^h = 0$  requires every token to lie in  $\ker(M_h)$ , which is a proper subspace under Condition 7. Generic tokens on  $S^{d-1}$  do not all lie there, so  $\|f_i^h\| > 0$  holds generically and is preserved along the flow. We exclude the degenerate set henceforth.

## 2.4 Standing Assumptions

Table 1 lists the conditions required by each main result. Conditions S and V are required throughout and define the gradient flow structure. All other conditions, including orthogonality (O, P), radial dominance ( $\tau$ ), scalar heads ( $M_h = \lambda_h I$ ), and equiangular/orthogonal token configurations, are imposed only in the theorems that explicitly list them. Results in Sections 7–11 are restricted to the scalar-head, equiangular-token regime and do not claim generality beyond that setting.

Table 1: Conditions required by each main result. “S, V” are required throughout. “Scalar” means  $M_h = \lambda_h I_d$ ; “equiangular” means all pairwise inner products  $\langle x_i, x_j \rangle$  are equal for  $i \neq j$ .

Result	Conditions	Regime
Thm 11 (total energy mono.)	S, V	General $M_h$ , general tokens
Thm 12 (approx. value)	S	General $M_h$ , general tokens
Thm 16 (flat per-head)	S, V, O, P	General $M_h$ (projection), general tokens
Thm 17 (sphere per-head)	S, V, O, P, $\tau$	General $M_h$ (projection), general tokens
Thm 19 (critical $\beta^*$ )	S, V, O, P, $\tau$	<b>Scalar heads, orthogonal tokens</b>
Thm 21 (normalized flow)	S, V	General $M_h$ , general tokens
Thm 22 (hetero. rates)	S, V	<b>Scalar heads, equiangular tokens</b>
Thm 25 (ReLU vs. softmax)	—	<b>Scalar heads, equiangular tokens, linearized</b>
Thm 27 (entropy identity)	S	General $M_h$ (any score-symmetric)
Cor 30 (entropy sign)	S	<b>Scalar heads, equiangular tokens</b>
Thm 39 (approx. orth.)	S, V	General $M_h$ , general tokens
Thm 40 (conv. rate)	S, V, O	<b>Scalar heads, equiangular tokens</b>

## 3 Total Energy Monotonicity

**Theorem 11** (Total Energy Monotonicity). (Requires: Conditions 3 and 4; general score matrices and token configurations.) *For both flat ( $\dot{x}_i = v_i$ ) and sphere ( $\dot{x}_i = P_{x_i}^\perp(v_i)$ ) dynamics:*

$$\frac{d\mathcal{E}_{\text{multi}}}{dt} = \frac{1}{n} \sum_{i=1}^n \|\dot{x}_i\|^2 \geq 0. \quad (5)$$

*Proof. Step 1: Differentiate each  $\mathcal{E}^h$  by the chain rule.* Fix a head  $h$ . Differentiating  $\mathcal{E}^h = \frac{1}{2\beta n^2} \sum_{i,j} e^{\beta \langle x_i, M_h x_j \rangle}$ :

$$\frac{d\mathcal{E}^h}{dt} = \frac{1}{2\beta n^2} \sum_{i,j} e^{\beta \langle x_i, M_h x_j \rangle} \cdot \beta \frac{d}{dt} \langle x_i, M_h x_j \rangle.$$

The  $\beta$  cancels with  $1/\beta$ . Since  $M_h$  is constant,  $\frac{d}{dt} \langle x_i, M_h x_j \rangle = \langle \dot{x}_i, M_h x_j \rangle + \langle x_i, M_h \dot{x}_j \rangle$ , so:

$$\frac{d\mathcal{E}^h}{dt} = \frac{1}{2n^2} \sum_{i,j} e^{\beta \langle x_i, M_h x_j \rangle} (\langle \dot{x}_i, M_h x_j \rangle + \langle x_i, M_h \dot{x}_j \rangle). \quad (6)$$

**Step 2: Symmetrize using Condition 3.** Write (6) as  $A + B$ . In  $B$ , swap  $i \leftrightarrow j$ :

$$B = \frac{1}{2n^2} \sum_{i,j} e^{\beta \langle x_j, M_h x_i \rangle} \langle x_j, M_h \dot{x}_i \rangle.$$

By Condition 3:  $\langle x_j, M_h x_i \rangle = \langle x_i, M_h x_j \rangle$  and  $\langle x_j, M_h \dot{x}_i \rangle = \langle \dot{x}_i, M_h x_j \rangle$ , so  $B = A$  and the  $1/2$  cancels:

$$\frac{d\mathcal{E}^h}{dt} = \frac{1}{n^2} \sum_i \left\langle \dot{x}_i, \underbrace{\sum_j e^{\beta \langle x_i, M_h x_j \rangle} M_h x_j}_{=f_i^h} \right\rangle = \frac{1}{n^2} \sum_i \langle \dot{x}_i, f_i^h \rangle. \quad (7)$$

**Step 3: Sum over heads and apply Condition 4.** Summing (7) over all  $H$  heads:

$$\frac{d\mathcal{E}_{\text{multi}}}{dt} = \frac{1}{n^2} \sum_i \left\langle \dot{x}_i, \sum_h f_i^h \right\rangle. \quad (8)$$

By (3),  $\sum_h f_i^h = n v_i$ , so:

$$\frac{d\mathcal{E}_{\text{multi}}}{dt} = \frac{1}{n} \sum_i \langle \dot{x}_i, v_i \rangle. \quad (9)$$

**Step 4a: Flat case** ( $\dot{x}_i = v_i$ ).

$$\frac{d\mathcal{E}_{\text{multi}}}{dt} = \frac{1}{n} \sum_i \|v_i\|^2 = \frac{1}{n} \sum_i \|\dot{x}_i\|^2 \geq 0.$$

**Step 4b: Sphere case** ( $\dot{x}_i = P_{x_i}^\perp(v_i)$ ). Substituting into (9) and applying Identity 1 with  $u = v_i$ :

$$\frac{d\mathcal{E}_{\text{multi}}}{dt} = \frac{1}{n} \sum_i \langle P_{x_i}^\perp(v_i), v_i \rangle = \frac{1}{n} \sum_i \|P_{x_i}^\perp(v_i)\|^2 = \frac{1}{n} \sum_i \|\dot{x}_i\|^2 \geq 0.$$

□

**Theorem 12** (Approximate Value Alignment). (Requires: Condition 3; builds on the chain-rule and symmetrization steps of Theorem 11; general score matrices and token configurations.) Suppose the value projections satisfy  $W^{V,h} = M_h + E_h$  with  $\|E_h\|_{\text{op}} \leq \varepsilon$  for all  $h$ . Define the perturbed aggregation  $\tilde{f}_i^h = \sum_j e^{\beta \langle x_i, M_h x_j \rangle} W^{V,h} x_j$ , the perturbed velocity  $\tilde{v}_i = \frac{1}{n} \sum_h \tilde{f}_i^h$ , and sphere dynamics  $\dot{x}_i = P_{x_i}^\perp(\tilde{v}_i)$ . Then:

$$\frac{d\mathcal{E}_{\text{multi}}}{dt} \geq \frac{1}{n} \sum_i \|\dot{x}_i\|^2 - \frac{\varepsilon}{n^2} \sum_i \|\dot{x}_i\| \sum_h \|\tilde{g}_i^h\|, \quad (10)$$

where  $\tilde{g}_i^h = \sum_j e^{\beta \langle x_i, M_h x_j \rangle} x_j$  is the unweighted aggregation. In particular,  $d\mathcal{E}_{\text{multi}}/dt \geq 0$  whenever

$$\varepsilon \leq \varepsilon^*(t) := \frac{\sum_i \|\dot{x}_i\|^2}{\frac{1}{n} \sum_i \|\dot{x}_i\| \sum_h \|\tilde{g}_i^h\|}.$$

*Proof. Step 1: Decompose the velocity.* Write  $\tilde{f}_i^h = f_i^h + e_i^h$  where  $e_i^h = E_h \tilde{g}_i^h$ , so  $\tilde{v}_i = v_i + \frac{1}{n} \sum_h e_i^h$ .

**Step 2: Energy derivative.** Steps 1–2 of Theorem 11 depend only on the score-matrix structure of  $\mathcal{E}^h$ , which is unchanged by the value perturbation. They give  $d\mathcal{E}_{\text{multi}}/dt = \frac{1}{n} \sum_i \langle \dot{x}_i, v_i \rangle$ .

**Step 3: Substitute the perturbed velocity.** Write  $v_i = \tilde{v}_i - \frac{1}{n} \sum_h e_i^h$ :

$$\frac{d\mathcal{E}_{\text{multi}}}{dt} = \frac{1}{n} \sum_i \langle \dot{x}_i, \tilde{v}_i \rangle - \frac{1}{n^2} \sum_i \sum_h \langle \dot{x}_i, e_i^h \rangle.$$

Identity 1 gives  $\langle \dot{x}_i, \tilde{v}_i \rangle = \|\dot{x}_i\|^2$ . Cauchy–Schwarz and  $\|e_i^h\| \leq \varepsilon \|\tilde{g}_i^h\|$  bound the second term.

**Step 4: Combine.**

$$\frac{d\mathcal{E}_{\text{multi}}}{dt} \geq \frac{1}{n} \sum_i \|\dot{x}_i\|^2 - \frac{\varepsilon}{n^2} \sum_i \|\dot{x}_i\| \sum_h \|\tilde{g}_i^h\|,$$

which is non-negative when  $\varepsilon \leq \varepsilon^*(t)$ .  $\square$

*Remark 13* (Interpretation of  $\varepsilon^*(t)$ ). The threshold  $\varepsilon^*(t)$  is the ratio of total kinetic energy to the perturbation’s leverage. It stays bounded away from zero as long as the dynamics have not halted. This parallels Theorem 39: both give monotonicity-under-small-perturbation results with explicit data-dependent thresholds. Together, they show the Lyapunov structure survives the two main idealizations in the model.

*Remark 14* (Sphere is slower than flat).  $\|\dot{x}_i\|_{\text{sphere}}^2 = \|P_{x_i}^\perp(v_i)\|^2 = \|v_i\|^2 - \langle v_i, x_i \rangle^2 \leq \|v_i\|^2 = \|\dot{x}_i\|_{\text{flat}}^2$ , with equality if and only if  $v_i \perp x_i$ . Both rates are non-negative; the sphere version is smaller because the tangential projection removes the radial part.

*Remark 15* (Wasserstein gradient flow). The identity  $d\mathcal{E}_{\text{multi}}/dt = \frac{1}{n} \sum_i \|\dot{x}_i\|^2$  identifies the dynamics as Wasserstein gradient ascent of  $\mathcal{F}[\mu] = \sum_h \frac{1}{2\beta} \iint e^{\beta \langle x, M_h y \rangle} d\mu(x) d\mu(y)$  in the sense of [1]. The first variation, evaluated at  $\mu = \frac{1}{n} \sum_j \delta_{x_j}$ , gives  $v_i$ . This is a restatement of Theorem 11, not an independent result.

## 4 Per-Head Energy Monotonicity

The total energy grows monotonically, but individual heads can fail to do so:

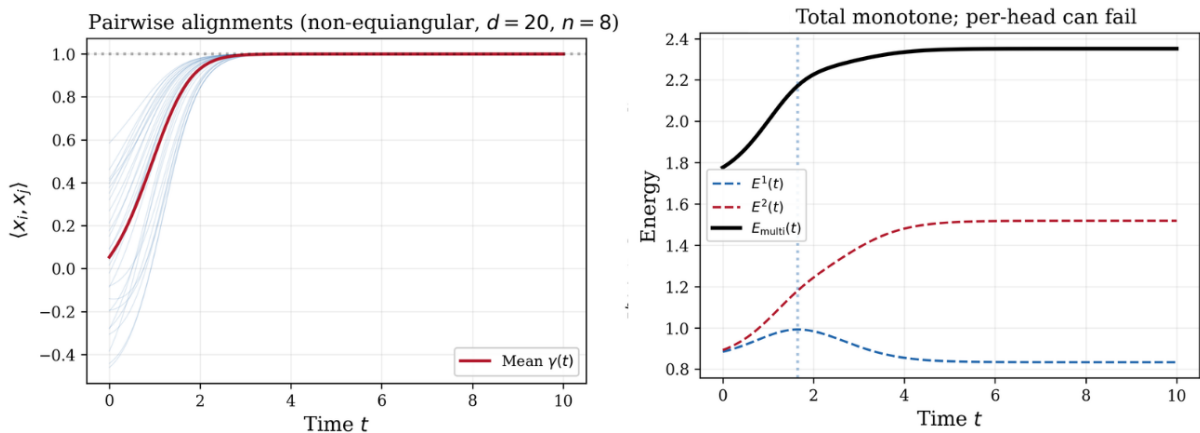


Figure 1: Alignment and energy dynamics in the non-equiangular regime. *Left*: Pairwise alignments  $\langle x_i, x_j \rangle$  over time for  $d = 20, n = 8$ . Individual trajectories (light blue) converge rapidly, while the mean alignment  $\gamma(t)$  (red) grows monotonically. *Right*: Per-head energies  $E^1(t)$  (blue, dashed) and  $E^2(t)$  (red, dashed), alongside  $E_{\text{multi}}(t)$  (black). Individual heads can be non-monotone while the total is monotone, illustrating that the Lyapunov structure is global. The vertical dashed line marks the transition where head-wise dynamics diverge.

The figure shows that individual heads can temporarily decrease while the sum grows. Monotonicity is a global property, not a head-by-head one. We now make this precise.

## 4.1 Flat Space

**Theorem 16** (Flat Per-Head Monotonicity). (Requires: Conditions 3, 4, 6, 7; general token configurations; builds on Step 2 of Theorem 11.) *Assume  $M_h \succeq 0$  for each  $h$ . Then:*

$$\frac{d\mathcal{E}^h}{dt} = \frac{1}{n^3} \sum_{i=1}^n \|f_i^h\|^2 \geq 0. \quad (11)$$

*Proof.* From (7),  $\frac{d\mathcal{E}^h}{dt} = \frac{1}{n^2} \sum_i \langle \dot{x}_i, f_i^h \rangle$ . In flat space,  $\dot{x}_i = v_i = \frac{1}{n} \sum_{h'} f_i^{h'}$ . Under Condition 7,  $M_{h'} f_i^{h'} = f_i^{h'}$ , so substituting:

$$\frac{d\mathcal{E}^h}{dt} = \frac{1}{n^3} \sum_i \sum_{h'} (f_i^{h'})^\top M_{h'} f_i^h. \quad (12)$$

*Cross terms ( $h' \neq h$ ):* Since  $f_i^h = M_h w_i^h$  where  $w_i^h = \sum_j e^{\beta \langle x_i, M_h x_j \rangle} x_j$ , Condition 6 gives  $M_{h'} f_i^h = M_{h'} M_h w_i^h = 0$ . So  $(f_i^{h'})^\top M_{h'} f_i^h = 0$ .

*Self term ( $h' = h$ ):*  $(f_i^h)^\top f_i^h = \|f_i^h\|^2 \geq 0$ .

Thus  $\frac{d\mathcal{E}^h}{dt} = \frac{1}{n^3} \sum_i \|f_i^h\|^2 \geq 0$ .  $\square$

## 4.2 Sphere — The Radial Shadow Obstruction

On the sphere, Condition 6 is not enough. Even with  $M_{h'} M_h = 0$  exactly, scalar projections of cross-head outputs onto  $x_i$  survive and interfere. We call these *radial shadows*. The theorem below identifies this precisely.

**Theorem 17** (Sphere Per-Head Monotonicity). (Requires: Conditions 3, 4, 6, 7, 8; general token configurations; extends Theorem 16 to sphere dynamics.)

$$\frac{d\mathcal{E}^h}{dt} = \frac{1}{n^3} \sum_i (b_i^h)^2 - \frac{1}{n^3} \sum_i a_i^h \sum_{h' \neq h} a_i^{h'} \geq 0. \quad (13)$$

*The bound holds on  $[0, T_{\text{crit}})$ , the interval during which Condition 8 is satisfied. Since  $\rho_i^h \rightarrow 1$  as  $\gamma \rightarrow 1$  and  $c^*(H) < 1$  for all  $H \geq 2$ , Condition 8 eventually fails; see Remark 42 and Open Problem 1.*

*Proof.* Four steps: reduce to an inner product against  $P_{x_i}^\perp(f_i^h)$ , evaluate cross-head terms, evaluate the self term, bound the interference.

**Step 1: Reduction via projection transfer.** From (7) and  $\dot{x}_i = P_{x_i}^\perp(v_i)$  with  $v_i = \frac{1}{n} \sum_{h'} M_{h'} f_i^{h'}$  (using Condition 7):

$$\frac{d\mathcal{E}^h}{dt} = \frac{1}{n^3} \sum_i \left\langle P_{x_i}^\perp \left( \sum_{h'} M_{h'} f_i^{h'} \right), f_i^h \right\rangle.$$

Apply Identity 2 to transfer the projection to the second argument:

$$\frac{d\mathcal{E}^h}{dt} = \frac{1}{n^3} \sum_i \sum_{h'} \langle M_{h'} f_i^{h'}, P_{x_i}^\perp(f_i^h) \rangle. \quad (14)$$

Expand  $P_{x_i}^\perp(f_i^h) = f_i^h - a_i^h x_i$  (using the radial component  $a_i^h = \langle f_i^h, x_i \rangle$ ):

$$\frac{d\mathcal{E}^h}{dt} = \frac{1}{n^3} \sum_i \sum_{h'} \underbrace{\langle M_{h'} f_i^{h'}, f_i^h \rangle}_{(A)} - a_i^h \underbrace{\langle M_{h'} f_i^{h'}, x_i \rangle}_{(B)}. \quad (15)$$

**Step 2: Cross-head terms** ( $h' \neq h$ ).

*Term (A):*  $(f_i^{h'})^\top M_{h'} f_i^h = (f_i^{h'})^\top M_{h'} M_h w_i^h = 0$  by Condition 6.

*Term (B):* By Condition 3 and  $f_i^{h'} \in \text{Im}(M_{h'})$ :  $\langle M_{h'} f_i^{h'}, x_i \rangle = \langle f_i^{h'}, x_i \rangle = a_i^{h'}$ .

So each cross-head summand contributes  $0 - a_i^h \cdot a_i^{h'} = -a_i^h a_i^{h'}$ .

**Step 3: Self term** ( $h' = h$ ). By Condition 7,  $M_h f_i^h = f_i^h$ , so  $\langle M_h f_i^h, P_{x_i}^\perp(f_i^h) \rangle = \langle f_i^h, P_{x_i}^\perp(f_i^h) \rangle = \|P_{x_i}^\perp(f_i^h)\|^2 = (b_i^h)^2$  by Identity 1.

**Assembling.**

$$\frac{d\mathcal{E}^h}{dt} = \frac{1}{n^3} \sum_i (b_i^h)^2 - \frac{1}{n^3} \sum_i a_i^h \sum_{h' \neq h} a_i^{h'}. \quad (16)$$

**Step 4: Bounding the interference.** By the triangle inequality and Condition 8:

$$\frac{1}{n^3} \sum_i |a_i^h| \sum_{h' \neq h} |a_i^{h'}| \leq \frac{1}{n^3} \sum_i |a_i^h| \cdot \frac{(b_i^h)^2}{\|f_i^h\|} = \frac{1}{n^3} \sum_i \rho_i^h (b_i^h)^2 \leq \frac{1}{n^3} \sum_i (b_i^h)^2.$$

So  $\frac{d\mathcal{E}^h}{dt} \geq \frac{1}{n^3} \sum_i (1 - \rho_i^h) (b_i^h)^2 \geq 0$ .  $\square$

*Remark 18* (The radial shadow obstruction). Condition 6 kills the operator-level term  $M_{h'} M_h = 0$ . However, it is unable to kill  $a_i^{h'} = \langle f_i^{h'}, x_i \rangle$ , since  $x_i$  is not constrained to  $\text{Im}(M_{h'})^\perp$ . These radial shadows, projections of each head's output onto the token position, survive regardless of how orthogonal the head subspaces are. Condition 8 is the precise requirement that the sum of these shadows does not exceed the head's own tangential power.

## 5 Critical Temperature Threshold

### 5.1 The Critical Alignment Fraction $c^*(H)$

In the uniform regime where all heads have alignment  $\rho_i^h = \rho$ , Condition 8 simplifies to  $(H-1)\rho \leq 1 - \rho^2$ , i.e.,

$$\rho^2 + (H-1)\rho - 1 \leq 0. \quad (17)$$

The positive root is

$$c^*(H) = \frac{\sqrt{(H-1)^2 + 4} - (H-1)}{2}. \quad (18)$$

For  $H = 2$ :  $c^*(2) = (\sqrt{5} - 1)/2 = 1/\varphi$ . For  $H = 3$ :  $c^*(3) = \sqrt{2} - 1$ .

**Theorem 19** (Critical Temperature). (Requires: Conditions 3, 4, 6, 7, 8; builds on the radial shadow analysis of Theorem 17; **restricted to scalar heads** ( $M_h = \alpha I_d$ ) **and orthogonal tokens**.)

For  $M_h = \alpha I_d$  ( $\alpha > 0$ ) and  $n$  mutually orthogonal tokens, Condition 8 holds if and only if  $\beta \leq \beta^*$ , where

$$\beta^* = \frac{1}{2\alpha} \ln \frac{c^*(H)^2(n-1)}{1 - c^*(H)^2}, \quad \text{requiring } n > 1/c^*(H)^2. \quad (19)$$

*Proof. Step 1: Compute the aggregation.* For  $M_h = \alpha I_d$  and  $\langle x_i, x_j \rangle = \delta_{ij}$ :

$$f_i^h = \alpha \left( e^{\alpha\beta} x_i + \sum_{j \neq i} x_j \right).$$

**Step 2: Compute the radial component.**  $a_i^h = \langle f_i^h, x_i \rangle = \alpha e^{\alpha\beta}$ , since the self-pairing gives 1 and the off-diagonal terms vanish by orthogonality.

**Step 3: Compute  $\|f_i^h\|$ .**  $\|f_i^h\|^2 = \alpha^2 (e^{2\alpha\beta} + n - 1)$ , so  $\|f_i^h\| = \alpha \sqrt{e^{2\alpha\beta} + n - 1}$ .

**Step 4: Compute  $\rho_i^h$  (the alignment fraction).**

$$\rho_i^h = \frac{|a_i^h|}{\|f_i^h\|} = \frac{e^{\alpha\beta}}{\sqrt{e^{2\alpha\beta} + n - 1}}.$$

**Step 5: Solve  $\rho_i^h = c^*(H)$ .** Set  $s = e^{\alpha\beta}$  (the self-attention Boltzmann weight). Then  $s/\sqrt{s^2 + n - 1} = c^*(H)$ . Squaring:  $s^2 = c^*(H)^2(n - 1)/(1 - c^*(H)^2)$ . Taking logarithms gives (19). □

*Remark 20* (Scope of scalar and equiangular assumptions). Theorems 19, 22, and 40 all rely on scalar score matrices  $M_h = \lambda_h I_d$  and/or equiangular/orthogonal token configurations. Scalar heads collapse the geometry to a single parameter; equiangular tokens reduce the full  $n$ -token ODE on  $S^{d-1}$  to a scalar ODE in  $\gamma$ . Both are strong idealizations. Extending the closed-form  $\beta^*$ , the super-additivity threshold  $\lambda_c$ , and the exponential convergence rate to general  $M_h$  and non-equiangular tokens is an important open direction.

## 6 Normalized Flow and Log-Partition Obstruction

**Theorem 21** (Normalized Flow). (Requires: Conditions 3 and 4; general score matrices and token configurations; builds on Theorem 11.) *Let  $Z_i^h = \sum_j e^{\beta\langle x_i, M_h x_j \rangle}$  (the normalizing constant for head  $h$  at token  $i$ ) and  $Z_i = \sum_h Z_i^h$ . Under normalized dynamics  $\dot{x}_i = P_{x_i}^\perp(v_i/Z_i)$ :*

$$\frac{d\mathcal{E}_{\text{multi}}}{dt} = \frac{1}{n} \sum_i Z_i \|\dot{x}_i\|^2 \geq 0. \quad (20)$$

The log-partition energy  $G = \frac{1}{\beta n} \sum_i \log Z_i$  generally does not have a monotone derivative.

*Proof. Monotonicity.* Steps 1–2 of Theorem 11 are unchanged, so (9) holds. With  $\dot{x}_i = P_{x_i}^\perp(v_i/Z_i)$ , apply Identity 2 then Identity 1:

$$\langle P_{x_i}^\perp(v_i/Z_i), v_i \rangle = \frac{1}{Z_i} \|P_{x_i}^\perp(v_i)\|^2 = Z_i \|\dot{x}_i\|^2.$$

Summing gives (20).

*Failure of  $G$ .* Differentiating  $G$  and swapping summation indices shows the derivative involves row-weighted aggregates  $\hat{f}_i = \sum_h \sum_j A_{ij}^h M_h x_j$  and column-weighted aggregates  $\tilde{f}_i = \sum_h \sum_j A_{ji}^h M_h x_j$  where  $A_{ij}^h = e^{\beta\langle x_i, M_h x_j \rangle}/Z_i$ . Since  $A_{ij}^h \neq A_{ji}^h$  whenever  $Z_i \neq Z_j$ , the sign of  $dG/dt$  is indefinite. □

## 7 Heterogeneous Head Convergence Rates

**Theorem 22** (Heterogeneous Scalar Head Rates). (Requires: Conditions 3, 4; **restricted to scalar heads  $M_h = \lambda_h I_d$  and equiangular token configurations**; see Remark 20.)

For  $M_h = \lambda_h I_d$  ( $\lambda_h > 0$  distinct) with  $\Lambda = \sum_h \lambda_h$ , in the equiangular reduction  $\gamma = \langle x_i, x_j \rangle$  ( $i \neq j$ ) with  $\varepsilon = 1 - \gamma$ :

- (a) **Late-time:**  $\dot{\varepsilon} = -2\Lambda\varepsilon + O(\varepsilon^2)$ , giving  $\varepsilon(t) \sim Ce^{-2\Lambda t}$ .
- (b) **Early-time:**  $g^h(0) = 2\lambda_h/(e^{\lambda_h\beta} + n - 1)$ , maximized at  $\lambda^*\beta = 1 + W((n - 1)/e)$  where  $W$  is the Lambert  $W$ -function.
- (c) **Super-additivity:** The rate function  $\phi(\lambda) = 2\lambda/(e^{\lambda\beta} + n - 1)$  has inflection point  $\lambda_c > \lambda^*$  satisfying

$$(\lambda_c\beta - 2)e^{\lambda_c\beta} = (\lambda_c\beta + 2)(n - 1), \quad (21)$$

and is strictly concave on  $(0, \lambda_c)$  and strictly convex on  $(\lambda_c, \infty)$ . When the mean head strength  $\bar{\lambda} = \Lambda/H$  satisfies  $\bar{\lambda} > \lambda_c$ ,

$$\sum_h \phi(\lambda_h) > H\phi(\bar{\lambda})$$

for any distinct  $\lambda_1, \dots, \lambda_H$  with  $\sum_h \lambda_h = \Lambda$ . Heterogeneous heads cluster faster than equal heads at the same total strength.

*Remark 23* ( $\lambda^*$  is not the inflection point).  $\lambda^*$  maximizes  $\phi$  ( $\phi'(\lambda^*) = 0$ ), while  $\lambda_c$  is where  $\phi'' = 0$ . They cannot coincide for  $\lambda > 0$ . Numerically,  $\lambda_c/\lambda^* \approx 1.7$  for small  $n$ . The condition  $\bar{\lambda} > \lambda_c$  is sufficient but not necessary.

*Proof. Step 1: Equiangular ODE.* With  $M_h = \lambda_h I$  and all  $\langle x_i, x_j \rangle = \gamma$  for  $i \neq j$ , permutation equivariance reduces the  $n$ -token dynamics to a scalar ODE for  $\gamma$  (following the symmetry reduction of [9, 10] applied to each head independently). The combined driving force is  $\dot{\gamma} = \sum_h g^h(\gamma)$  where

$$g^h(\gamma) = \frac{2\lambda_h e^{\lambda_h \beta \gamma} (1 - \gamma)(1 + (n - 1)\gamma)}{e^{\lambda_h \beta} + (n - 1)e^{\lambda_h \beta \gamma}}. \quad (22)$$

*Remark 24* (Equiangular reduction). The reduction requires all pairwise inner products to be equal at  $t = 0$  and to remain so. Permutation equivariance of the ODE guarantees this is preserved if it holds initially. For non-equiangular data,  $\gamma$  becomes a vector of pairwise angles and the scalar ODE does not apply; Theorems 22 and 40 hold only on this symmetric submanifold.

**Step 2: Late-time expansion** ( $\varepsilon \rightarrow 0$ ). Set  $\gamma = 1 - \varepsilon$  (so  $\varepsilon$  measures distance to full clustering). To leading order,  $g^h(1 - \varepsilon) \approx 2\lambda_h \varepsilon$ . Summing:  $\dot{\varepsilon} = -2\Lambda\varepsilon + O(\varepsilon^2)$ , with solution  $\varepsilon(t) \sim Ce^{-2\Lambda t}$ .

**Step 3: Early-time rate at  $\gamma = 0$ .**  $g^h(0) = 2\lambda_h/(e^{\lambda_h \beta} + n - 1)$  by direct substitution.

**Step 4: Maximize over  $\lambda_h$ .** Setting  $\partial g^h(0)/\partial \lambda_h = 0$  gives  $(1 - \lambda^* \beta)e^{\lambda^* \beta} = -(n - 1)$ .

**Step 5: Lambert  $W$  form.** Let  $u = \lambda^* \beta - 1$ . Then  $ue^u = (n - 1)/e$ , so  $u = W((n - 1)/e)$  and  $\lambda^* \beta = 1 + W((n - 1)/e)$ .

**Step 6: Concavity–convexity structure.** Setting  $E = e^{\lambda \beta}$  and  $\sigma = E + n - 1$ :

$$\phi'(\lambda) = \frac{2((1 - \lambda\beta)E + n - 1)}{\sigma^2}, \quad \phi''(\lambda) = \frac{2\beta E[(\lambda\beta - 2)E - (\lambda\beta + 2)(n - 1)]}{\sigma^3}.$$

At  $\lambda^*$ ,  $\phi'(\lambda^*) = 0$  implies  $(1 - \lambda^* \beta)E^* = -(n - 1)$ ; substituting into the numerator of  $\phi''$  gives  $\phi''(\lambda^*) = -2(\lambda^* \beta)^2 \beta (E^*)^2 / \sigma^{*3} < 0$ , so  $\lambda^*$  is a strict maximum. The numerator of  $\phi''$  is negative at  $\lambda^*$  and grows without bound as  $\lambda \rightarrow \infty$ , so there is a unique  $\lambda_c > \lambda^*$  where it vanishes, giving the stated concavity/convexity.

**Step 7: Super-additivity via Jensen.** For  $\bar{\lambda} > \lambda_c$ , all  $\lambda_h$  near  $\bar{\lambda}$  lie in the convex region. Jensen's inequality gives  $\phi(\bar{\lambda}) \leq \frac{1}{H} \sum_h \phi(\lambda_h)$ , with strict inequality when the  $\lambda_h$  are not all equal. When some  $\lambda_h$  fall below  $\lambda_c$ , a Taylor expansion to third order and the bound  $|\phi'''(\lambda)| \leq 6\beta^2 \phi(\lambda)/\lambda$  give the quantitative sufficient condition

$$\max_h |D_h| < \frac{3\phi''(\bar{\lambda}) \min_h \lambda_h}{\beta^2 \max_h \phi(\lambda_h)},$$

where  $D_h = \lambda_h - \bar{\lambda}$ , under which super-additivity still holds.  $\square$

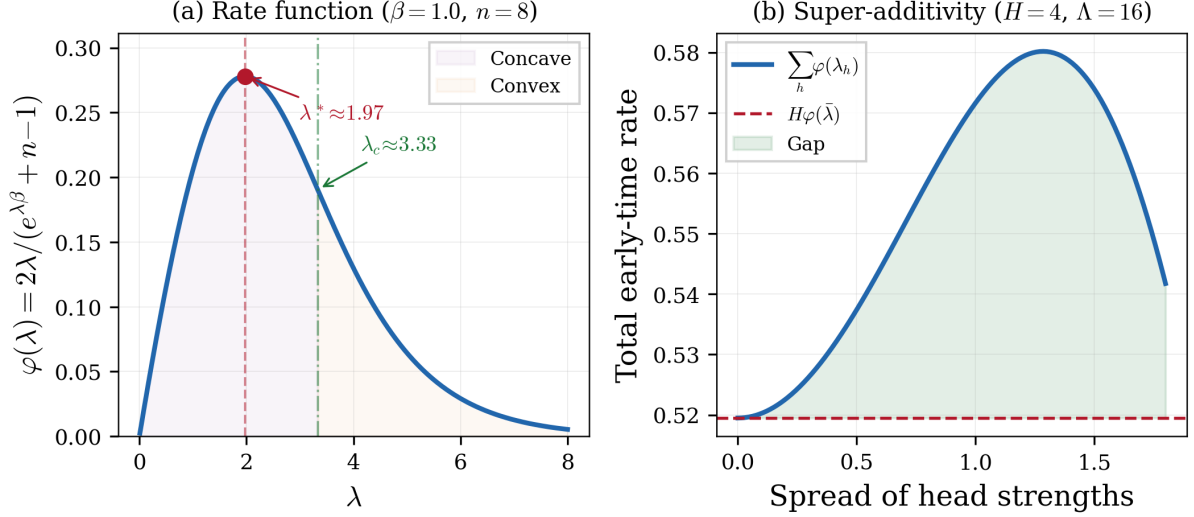


Figure 2: Rate function and super-additivity (Theorem 22). (a)  $\phi(\lambda) = 2\lambda/(e^{\lambda^\beta} + n - 1)$  with maximum  $\lambda^* \approx 1.97$  and inflection  $\lambda_c \approx 3.33$ . (b) For  $H = 4$  heads with  $\Lambda = 16$  in the convex regime ( $\bar{\lambda} = 4 > \lambda_c$ ), heterogeneous strengths strictly exceed equal strengths. Parameters:  $\beta = 1.0$ ,  $n = 8$ .

## 8 ReLU vs. Softmax Clustering Time

**Theorem 25** (Clustering Time Separation — Linearized Regime). (Requires: **scalar head**  $M = \lambda I$ , **equiangular-token reduction**, **linearized ODE near  $\gamma = 0$** ; builds on Theorem 22. The full nonlinear regime is deferred to Open Problem 5.)

For random tokens on  $S^{d-1}$  with  $\gamma_0 = O(1/\sqrt{d})$ , the following separation holds in the linearized regime near  $\gamma = 0$ :

- (a) **ReLU** ( $\sigma(t) = \max(0, t)$ ):  $\dot{\gamma} = (2\lambda^2/n)\gamma + O(\gamma^2)$  near  $\gamma = 0$ , giving  $T_{\text{ReLU}} = O(n \log d)$ .
- (b) **Softmax**:  $\dot{\gamma}|_{\gamma=0} = 2\lambda/(e^{\lambda^\beta} + n - 1) > 0$ , a positive constant independent of  $d$ , giving  $T_{\text{softmax}} = O(n)$ .

A complete proof for the nonlinear regime requires handling the non-smooth boundary  $\{\gamma = 0\}$  and the regime  $\gamma = \Omega(1)$ ; see Open Problem 5.

*Proof. Step 1: Initialization.* For  $x_i$  uniformly random on  $S^{d-1}$ ,  $\langle x_i, x_j \rangle \approx \mathcal{N}(0, 1/d)$  by the central limit theorem, so  $\gamma_0 = O(1/\sqrt{d})$  with high probability.

**Step 2: Softmax near  $\gamma = 0$ .** From Theorem 22,  $g^h(0) = c_0 = 2\lambda/(e^{\lambda^\beta} + n - 1) > 0$  independent of  $d$ . The ODE  $\dot{\gamma} \approx c_0 > 0$  gives  $\gamma(t) \approx \gamma_0 + c_0 t$ , so  $T_{\text{softmax}} = O(1/c_0) = O(n)$ .

**Step 3: ReLU equiangular ODE.** With  $M = \lambda I$ , the ReLU aggregation gives velocity  $v_i = (\lambda^2/n)[x_i + \gamma \sum_{j \neq i} x_j]$  when  $\gamma > 0$ . Computing  $\langle \dot{x}_i, x_j \rangle$  and factoring:

$$\dot{\gamma} = \frac{2\lambda^2\gamma}{n}(1 - \gamma)(1 + (n - 1)\gamma). \quad (23)$$

At  $\gamma = 0$ :  $\dot{\gamma} = 0$  since  $\text{ReLU}(0) = 0$ . Near  $\gamma = 0^+$ :  $\dot{\gamma} \approx (2\lambda^2/n)\gamma$ .

**Step 4: ReLU clustering time.** From the linearized ODE:  $\gamma(t) = \gamma_0 e^{2\lambda^2 t/n} = (C/\sqrt{d}) e^{2\lambda^2 t/n}$ . Setting  $\gamma(T) = \Omega(1)$ :  $T = O(n \log d)$ .  $\square$

*Remark 26* (Hybrid architectures). This is an informal comparison; a full version requires the nonlinear extension of Theorem 25. At early times, ReLU is completely silent at  $\gamma = 0$  while softmax drives everything. At late times, softmax heads carry a suppression factor  $e^{-\lambda_h \beta}$  from

over-concentration [21], while ReLU heads carry none, so even weak ReLU heads dominate late-time convergence at large  $\beta$ . This is consistent with the empirical finding that ReLU attention can match or approach softmax performance [20, ?].

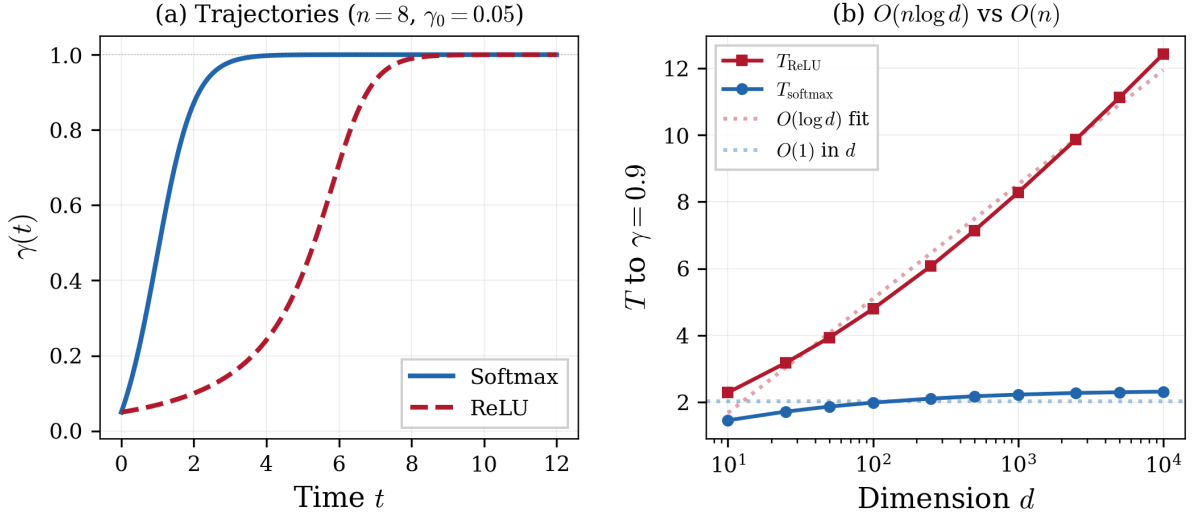


Figure 3: ReLU vs. softmax clustering time (Theorem 25). (a) Softmax reaches  $\gamma \approx 1$  roughly four times faster for  $n = 8$ ,  $\gamma_0 = 0.05$ . (b)  $T_{\text{ReLU}}$  grows as  $O(\log d)$  while  $T_{\text{softmax}}$  is  $O(1)$  in  $d$ , confirming the separation. Parameters:  $\lambda = 1.0$ ,  $\beta = 1.0$ ,  $n = 8$ .

## 9 Attention Entropy Production Identity

The normalized attention distribution for head  $h$  at token  $i$  is

$$p_{ij}^h = \frac{e^{\beta \langle x_i, M_h x_j \rangle}}{Z_i^h}, \quad Z_i^h = \sum_k e^{\beta \langle x_i, M_h x_k \rangle}, \quad H_i^h = - \sum_j p_{ij}^h \log p_{ij}^h.$$

**Theorem 27** (Entropy Production Identity). (Requires: Condition 3 only; valid for any score-symmetric attention and any sphere dynamics. The sign of the covariance is established in Corollary 30 for the scalar-head equiangular case.)

Write  $s_j = \langle x_i, M_h x_j \rangle$  (the score of token  $j$  from token  $i$  under head  $h$ ) and  $\dot{s}_j = \langle \dot{x}_i, M_h x_j \rangle + \langle M_h x_i, \dot{x}_j \rangle$ . Then:

$$\frac{dH_i^h}{dt} = -\beta^2 \text{Cov}_{p_i^h}(s_j, \dot{s}_j). \quad (24)$$

This is an exact identity. The sign of the covariance depends on the dynamics and is established separately.

*Proof.* Write  $Z = Z_i^h$ ,  $p_j = p_{ij}^h$ ,  $\mathbb{E}_p[\cdot] = \sum_j p_j(\cdot)$ .

**Step 1: Exponential-family decomposition.** Since  $\log p_j = \beta s_j - \log Z$ :

$$H_i^h = \log Z - \beta \mathbb{E}_p[s]. \quad (25)$$

**Step 2: Differentiate  $\log Z$ .**

$$\frac{d \log Z}{dt} = \beta \mathbb{E}_p[\dot{s}]. \quad (26)$$

**Step 3: Differentiate  $\mathbb{E}_p[s]$ .** Since  $\dot{p}_j = \beta p_j(\dot{s}_j - \mathbb{E}_p[\dot{s}])$ :

$$\frac{d}{dt} \mathbb{E}_p[s] = \beta \text{Cov}_p(s, \dot{s}) + \mathbb{E}_p[\dot{s}]. \quad (27)$$

**Step 4: Combine.**

$$\frac{dH_i^h}{dt} = \beta \mathbb{E}_p[\dot{s}] - \beta(\beta \text{Cov}_p(s, \dot{s}) + \mathbb{E}_p[\dot{s}]) = -\beta^2 \text{Cov}_p(s, \dot{s}).$$

**Step 5: Sign of  $\text{Cov}_p(s, \dot{s})$ .** Split  $\dot{s}_j = \dot{s}_j^I + \dot{s}_j^{II}$  where  $\dot{s}_j^I = \langle \dot{x}_i, Mx_j \rangle$  (token  $i$  moving) and  $\dot{s}_j^{II} = \langle Mx_i, \dot{x}_j \rangle$  (token  $j$  moving). In general, neither  $\text{Cov}_p(s, \dot{s}^I)$  nor  $\text{Cov}_p(s, \dot{s}^{II})$  vanishes individually. The sign of their sum  $\text{Cov}_p(s, \dot{s})$  depends on the dynamics and is established in Corollary 30 for the scalar-head equiangular case via a direct two-group calculation.

*Remark 28* (Component I in the scalar equiangular case). When  $M = \lambda I$  and tokens are equiangular,  $\dot{s}_j^I$  takes only two values (zero for  $j = i$  and a common positive constant for  $j \neq i$ ), and  $\text{Cov}_p(s, \dot{s}^I)$  is strictly negative, not zero. Both components contribute to the total covariance with the same sign. □

*Remark 29* (Information flow interpretation). The identity  $dH/dt = -\beta^2 \text{Cov}_p(s_j, \dot{s}_j)$  has a clean interpretation. Writing  $\text{Cov}_p(s, \dot{s}) = \mathbb{E}_p[(s - \mathbb{E}_p[s])\dot{s}]$ , the sign is determined by whether above-average score tokens tend to increase or decrease. If high-score tokens increase, attention sharpens and entropy falls. If they decrease, mass spreads and entropy rises. The formula makes this direction computable.

**Corollary 30** (Entropy monotonicity — equiangular case). (Requires: Condition 3; builds on Theorem 27 (Step 5); **restricted to scalar head  $M = \lambda I_d$  and equiangular configuration.**)

For a single head  $M = \lambda I_d$  and  $\langle x_j, x_k \rangle = \gamma$  ( $j \neq k$ ) with  $\gamma \in (0, 1)$ :

$$\text{Cov}_{p_i}(s_j, \dot{s}_j) \leq 0, \quad \text{so} \quad \frac{dH_i}{dt} \geq 0.$$

In the scalar-head equiangular regime, attention entropy is monotonically non-decreasing for all  $n \geq 2$ .

*Proof.* We compute  $\text{Cov}_p(s_j, \dot{s}_j)$  directly via the two-group structure of the equiangular scalar-head case.

**Step 1: Score and velocity structure.** Scores:  $s_i = \lambda$  (self) and  $s_j = \lambda\gamma$  for  $j \neq i$ . The softmax has two mass types:  $p_i = e^{\beta\lambda}/Z$  and  $p_j = e^{\beta\lambda\gamma}/Z$  for  $j \neq i$ .

**Step 2: Full score velocities.** Recall  $\dot{s}_j = \dot{s}_j^I + \dot{s}_j^{II}$  where  $\dot{s}_j^I = \langle \dot{x}_i, \lambda x_j \rangle$  and  $\dot{s}_j^{II} = \lambda \langle x_i, \dot{x}_j \rangle$ .

*Component II:* For  $j = i$ :  $\dot{s}_i^{II} = \lambda \langle x_i, \dot{x}_i \rangle = 0$  since  $\dot{x}_i \perp x_i$  on  $S^{d-1}$ . For  $j \neq i$ : by the equiangular reduction,  $\frac{d}{dt} \langle x_i, x_j \rangle = \dot{\gamma} = 2 \langle x_i, \dot{x}_j \rangle$ , so  $\dot{s}_j^{II} = \lambda \dot{\gamma}/2 =: c > 0$ .

*Component I:* For  $j = i$ :  $\dot{s}_i^I = \lambda \langle \dot{x}_i, x_i \rangle = 0$  since  $\dot{x}_i \perp x_i$ . For  $j \neq i$ : by equiangular symmetry,  $\langle \dot{x}_i, x_j \rangle$  is the same constant  $c'$  for all  $j \neq i$ . Since  $\dot{\gamma} = \langle \dot{x}_i, x_j \rangle + \langle x_i, \dot{x}_j \rangle = c' + c/\lambda$ , we have  $c' = \dot{\gamma} - c/\lambda$ . So  $\dot{s}_j^I = \lambda c'$  for  $j \neq i$ .

*Total:*  $\dot{s}_i = 0$  and  $\dot{s}_j = \lambda c' + c$  for  $j \neq i$ . Both values are positive constants during clustering.

**Step 3: Two-group covariance.** The joint distribution takes two values:  $(s_i, \dot{s}_i) = (\lambda, 0)$  with weight  $p_i$  and  $(s_j, \dot{s}_j) = (\lambda\gamma, \lambda c' + c)$  with total weight  $1 - p_i$ . The two-group covariance formula gives:

$$\text{Cov}_p(s, \dot{s}) = p_i(1 - p_i) \cdot \lambda(1 - \gamma) \cdot (-\lambda c' + c) < 0.$$

Each factor is positive for  $\gamma \in (0, 1)$  and  $n \geq 2$  (since  $\lambda c' + c = \lambda \dot{\gamma} > 0$  during clustering), so the covariance is strictly negative and  $dH_i/dt = -\beta^2 \text{Cov}_p(s, \dot{s}) > 0$ . □

*Remark 31* (Physical interpretation). The anti-monotone pairing is forced by the sphere: the highest score (self-score  $\lambda$ ) is paired with zero velocity ( $\dot{s}_i^{II} = 0$ ) because tangential motion cannot change  $\langle x_i, x_i \rangle = 1$ . Lower cross-scores are paired with positive velocity. As tokens cluster, all pairwise scores equalize toward  $\lambda$ , softmax converges to uniform, and entropy rises to  $\log n$ .

*Remark 32* (Entropy sign beyond the scalar case). The cancellation  $\dot{s}_i^{II} = 0$  relies on  $Mx_i \propto x_i$ , which holds when  $M = \lambda I$ . For general symmetric  $M \succeq 0$ , this fails and  $\text{Cov}_p(s_j, \dot{s}_j)$  need not be non-positive. Numerical experiments show it can become positive along the flow. The identity (24) remains exact; only the sign is regime-dependent.

**Lemma 33** (Cross-head covariance). (Requires: Conditions 3, 4, 6, 7; extends the Component I analysis of Theorem 27 to the multi-head setting.) For head  $h$  and token  $i$ , let  $A_h^{(i)} = \sum_{h' \neq h} a_i^{h'}$  (total radial shadow from other heads). Then

$$\text{Cov}_{p_i^h}(s_j, \dot{s}_j^I) = -\frac{A_h^{(i)}}{n} \text{Var}_{p_i^h}(s_j).$$

*Proof.* Decompose  $\dot{x}_i = \dot{x}_i^{(h)} + \dot{x}_i^{(-h)}$  where  $\dot{x}_i^{(h)} = \frac{1}{n} P_{x_i}^\perp(f_i^h)$  and  $\dot{x}_i^{(-h)} = \frac{1}{n} \sum_{h' \neq h} P_{x_i}^\perp(f_i^{h'})$ .

For the cross part, Identity 2 and Conditions 7, 6 give  $\langle P_{x_i}^\perp(f_i^{h'}), M_h x_j \rangle = -s_j a_i^{h'}$ . The self part  $\dot{x}_i^{(h)}$  contributes  $\text{Cov}_{p_i^h}(s_j, \langle \dot{x}_i^{(h)}, M_h x_j \rangle)$ , which need not vanish in general (see Remark 28). The stated formula captures the cross-head contribution: summing over  $h' \neq h$  and taking the covariance gives  $\text{Cov}_{p_i^h}(s_j, -(s_j/n)A_h^{(i)}) = -(A_h^{(i)}/n)\text{Var}_{p_i^h}(s_j)$ .  $\square$

**Proposition 34** (Multi-head entropy decomposition). (Requires: Conditions 3, 4, 6, 7; builds on Theorem 27 and Lemma 33.) For  $H \geq 2$ :

$$\frac{dH_i^h}{dt} = -\frac{\beta^2}{n} \text{Cov}_{\text{single}} + \frac{\beta^2 A_h^{(i)}}{n} \text{Var}(s_j) + \frac{\beta^2}{n} \sum_{h' \neq h} \text{Cov}_{p_i^h}(s_j, a_j^{h'} s_j).$$

The right-hand side is  $\leq 0$  whenever:

$$\text{Cov}_{\text{single}}(s_j, \dot{s}_j^{\text{II},h}) \geq A_h^{(i)} \text{Var}(s_j) + \sum_{h' \neq h} \text{Cov}_{p_i^h}(s_j, a_j^{h'} s_j). \quad (\text{Condition E})$$

*Remark 35* (When Condition E holds). In Phase 1 (pre-clustering),  $A_h^{(i)} \approx 0$  by approximate cross-head orthogonality and the cross-covariance terms are small. Condition E then reduces to  $\text{Cov}_{\text{single}} \leq 0$ , which holds in the equiangular scalar-head case by Corollary 30 but not for general  $M$  (Remark 32). In Phase 2,  $\dot{s}_j \rightarrow 0$  and both sides vanish. The intermediate regime remains the main open case.

## 9.1 Two-Phase Structure of Entropy Dynamics

*Remark 36* (Phase 1: Pre-clustering). When  $\gamma \ll 1$ , the self-score  $s_i = \lambda$  dominates the cross-scores  $s_j = \lambda\gamma$ . Cross-score velocities  $\dot{s}_j$  are large and positive as tokens approach each other, while  $\dot{s}_i = 0$  by the sphere constraint. This anti-monotone pairing drives  $dH_i^h/dt \gg 0$ : entropy rises quickly as attention spreads from peaked toward uniform.

*Remark 37* (Phase 2: Near full clustering). As  $\gamma \rightarrow 1$ , all pairwise scores equalize,  $p_{ij}^h \rightarrow 1/n$ , and  $\dot{s}_j \rightarrow 0$ . So  $\text{Cov}_p(s, \dot{s}) \rightarrow 0$  and  $dH_i^h/dt \rightarrow 0$ : entropy stabilizes at  $\log n$ .

*Remark 38* (Why entropy increases, not decreases). It may seem like tokens clustering together should sharpen attention and decrease entropy. That would be right if clustering were selective, with some tokens approaching while others stayed distant. However, the gradient flow produces a single-cluster collapse where all tokens approach equally. All pairwise scores equalize, softmax converges to uniform, and entropy increases. The formula  $dH_i^h/dt = -\beta^2 \text{Cov}_p(s, \dot{s})$  captures this exactly. Entropy stabilizes only when all scores equalize and the dynamics halt.

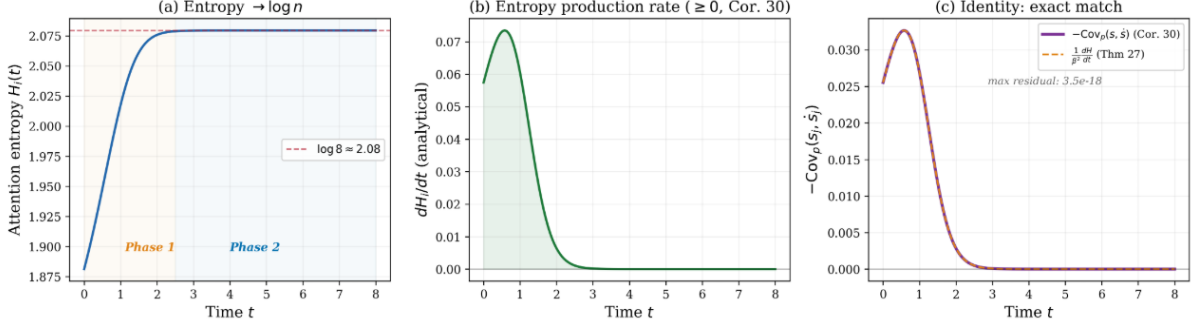


Figure 4: Entropy production identity and two-phase structure (Theorem 27, Corollary 30). (a)  $H_i(t)$  increases toward  $\log n$  in two phases. (b)  $dH_i/dt \geq 0$  peaks during pre-clustering and vanishes at equilibrium. (c) The identity  $dH/dt = -\beta^2 \text{Cov}_p(s_j, \dot{s}_j)$  holds to machine precision (max residual  $3 \times 10^{-18}$ ). Parameters:  $M = \lambda I$ ,  $\lambda = 1.0$ ,  $\beta = 1.5$ ,  $n = 8$ ,  $\gamma_0 = 0.05$ .

## 10 Approximate Head Orthogonality

Condition 6 is never exactly satisfied in trained transformers. Empirical principal angles between Q/K subspaces are 70–85°, not 90°. We relax it to  $\|M_{h'} M_h\|_{\text{op}} \leq \delta$ .

**Theorem 39** (Approximate Orthogonality). (Requires: Conditions 3, 4, and  $\|M_{h'} M_h\|_{\text{op}} \leq \delta$  for all  $h' \neq h$ ; flat dynamics; general token configurations; extends Theorem 16 to approximately orthogonal heads.)

In the flat case:

$$\frac{d\mathcal{E}^h}{dt} \geq \frac{1}{n^3} \left( \sum_i (f_i^h)^\top M_h f_i^h - \delta' \sum_i \|f_i^h\| \sum_{h' \neq h} \|f_i^{h'}\| \right) \geq 0 \quad (28)$$

whenever  $\delta' \leq \delta^*(t)$ , where

$$\delta' = \frac{\delta}{\sigma_{\min}(M_h)}, \quad \delta^*(t) = \frac{\sum_i (f_i^h)^\top M_h f_i^h}{\sum_i \|f_i^h\| \sum_{h' \neq h} \|f_i^{h'}\|},$$

and  $\sigma_{\min}(M_h) > 0$  is the smallest nonzero singular value of  $M_h$ .

*Proof.* From (12),  $\frac{d\mathcal{E}^h}{dt} = \frac{1}{n^3} \sum_i \sum_{h'} (f_i^{h'})^\top M_{h'} f_i^h$ .

*Self term:*  $(f_i^h)^\top M_h f_i^h \geq 0$ .

*Cross terms:* Write  $w_i^h = \sum_j e^{\beta \langle x_i, M_h x_j \rangle} x_j$ , so  $f_i^h = M_h w_i^h$  where  $w_i^{h, \parallel} \in \text{row}(M_h)$ . Then:

$$|(f_i^{h'})^\top M_{h'} f_i^h| \leq \|f_i^{h'}\| \cdot \delta \cdot \|w_i^{h, \parallel}\| \leq \delta' \|f_i^{h'}\| \|f_i^h\|,$$

using  $\|w_i^{h, \parallel}\| \leq \|f_i^h\| / \sigma_{\min}(M_h)$  and  $\delta' = \delta / \sigma_{\min}(M_h)$ . Summing and applying the triangle inequality gives (28).  $\square$

## 11 Sharp Per-Head Convergence Rate Near Equilibrium

**Theorem 40** (Per-Head Exponential Convergence). (Requires: Conditions 3, 4, 6; builds on the late-time expansion of Theorem 22(a); **restricted to scalar heads  $M_h = \lambda_h I_d$  and equian-gular tokens.**)

With  $\Lambda = \sum_h \lambda_h$  and  $\Delta\mathcal{E}^h = \mathcal{E}^{h*} - \mathcal{E}^h(t)$  near the clustered equilibrium ( $\varepsilon = 1 - \gamma \rightarrow 0$ ):

$$\Delta\mathcal{E}^h(t) \leq C_h \exp(-2\Lambda t), \quad (29)$$

where  $C_h = \frac{(n-1)\lambda_h}{2n} e^{\beta\lambda_h} \varepsilon_0$ .

*Proof. Step 1: Energy gap in terms of  $\varepsilon$ .* For diagonal score  $\lambda_h$  and off-diagonal score  $\lambda_h(1 - \varepsilon)$ , expanding around  $\varepsilon = 0$ :

$$\Delta\mathcal{E}^h \approx \frac{(n-1)\lambda_h}{2n} e^{\beta\lambda_h} \varepsilon.$$

**Step 2: ODE for  $\varepsilon$ .** From Theorem 22(a):  $\varepsilon(t) \approx \varepsilon_0 e^{-2\Lambda t}$ .

**Step 3: Combine.**  $\Delta\mathcal{E}^h(t) \leq C_h e^{-2\Lambda t}$  with  $C_h = \frac{(n-1)\lambda_h}{2n} e^{\beta\lambda_h} \varepsilon_0$ .

*Remark 41* (Normalized vs. unnormalized near equilibrium). Bound (29) comes from normalized dynamics (22). For unnormalized dynamics (3), the factor  $(1 + (n-1)\gamma) \rightarrow n$  near equilibrium exactly cancels the  $1/n$  prefactor, giving rate  $2 \sum_h \lambda_h e^{\beta\lambda_h}$  instead of  $2\Lambda$ . The cancellation is geometric, not due to normalization. □

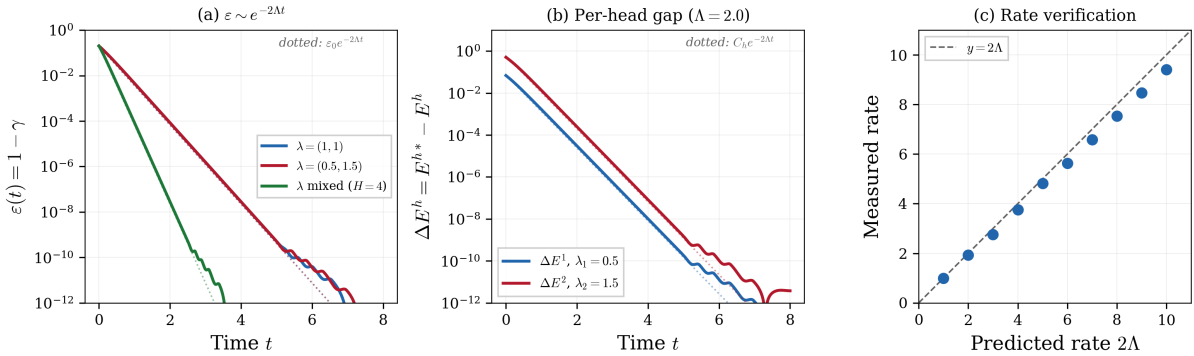


Figure 5: Exponential convergence near equilibrium (Theorem 40). (a)  $\varepsilon(t) = 1 - \gamma(t)$  decays at rate  $2\Lambda$  (dotted:  $\varepsilon_0 e^{-2\Lambda t}$ ). (b) Per-head energy gap  $\Delta E^h$  for  $\lambda_1 = 0.5$ ,  $\lambda_2 = 1.5$  at shared rate  $2\Lambda = 4$ . (c) Measured rates vs.  $2\Lambda$  across a range of total strengths. All:  $n = 8$ ,  $\beta = 1.0$ ,  $\gamma_0 = 0.8$ .

## 12 Conclusion

We have built a rigorous framework for multi-head self-attention as a gradient flow on the unit sphere, extending the single-head theory of [9, 10].

The central finding is the radial shadow: a cross-head interference term in the per-head energy derivative that survives even when head subspaces are exactly orthogonal. Total energy  $\mathcal{E}_{\text{multi}}$  is monotone unconditionally (Theorem 11). Per-head monotonicity requires the Radial Dominance condition (Condition 8), which holds precisely when  $\beta \leq \beta^*$ , a threshold we compute in closed form via the golden ratio and Lambert  $W$ -function in the scalar-head, orthogonal-token regime (Theorem 19).

The remaining quantitative results are all in the scalar-head, equiangular-token regime (see Remark 20 and Table 1). Theorem 22 shows that spreading head strengths strictly improves early-time clustering when the mean strength is in the convex regime of the rate function. Theorem 25 gives a rigorous basis, in the linearized regime, for the observation that ReLU and

softmax have complementary strengths: softmax drives clustering from  $\gamma = 0$  while ReLU is silent there, but ReLU dominates at late times when softmax over-concentrates. The entropy identity (Theorem 27) and its sign result (Corollary 30) make the two-phase dynamics precise: entropy increases during pre-clustering as scores equalize and attention spreads, then stabilizes at  $\log n$ .

The main open questions are the behavior after  $T_{\text{crit}}$  (Open Problem 1), the structure of critical points of the multi-head flow (Open Problem 2), and the sign of  $\text{Cov}_p(s_j, \dot{s}_j)$  for general score matrices, where entropy monotonicity need not hold (Remark 32).

## 13 Open Problems

*Open Problem 1* (Trajectory-invariance of Condition 8). Per-head monotonicity holds only on  $[0, T_{\text{crit}}]$ . Since  $\rho_i^h \rightarrow 1 > c^*(H)$  as  $\gamma \rightarrow 1$ , Condition 8 eventually fails for any  $H \geq 2$ . Is there a natural class of initial conditions for which the trajectory stays in the  $\tau$ -satisfying region long enough to conclude clustering? The entropy production rate  $\beta^2 \text{Cov}_p(s_j, \dot{s}_j)$  controls how quickly  $\rho_i^h$  grows, and could yield a lower bound on  $T_{\text{crit}}$ , though bounding  $\dot{\rho}_i^h$  in terms of  $dH_i^h/dt$  directly remains open. This is also related to the metastability studied in [8] and [3].

*Remark 42* ( $T_{\text{crit}}$  bound).  $T_{\text{crit}} = \inf\{t : \rho_i^h(t) = c^*(H)\}$ . Since  $\rho_i^h$  satisfies a nonlinear ODE coupled to the full token dynamics, a closed-form lower bound requires controlling  $\dot{\rho}_i^h$  independently of the entropy. The entropy plateau (Phase 2) and the  $\rho = c^*(H)$  crossing are distinct events that need not coincide. A quantitative  $T_{\text{crit}}$  bound remains open.

*Open Problem 2* (Critical points of the multi-head flow). The Lyapunov structure shows  $\mathcal{E}_{\text{multi}}$  increases but does not show that trajectories converge to full clusters. This requires showing all stable critical points are complete clusters. For single-head flows, [10] does this via a cone-collapse argument; whether it extends to the combined velocity field  $\frac{1}{n} \sum_h f_i^h$  is open.

*Open Problem 3* (Per-head Wasserstein structure). No single positive-definite metric  $G_i$  satisfies  $G_i \dot{x}_i = (1/n^2) u_i^h$  for all  $h$  simultaneously. A head-indexed family of metrics  $\{G^h\}$  under which each  $\mathcal{F}^h$  is a gradient flow is being investigated via the Wasserstein–Fisher–Rao framework [6].

*Open Problem 4* (Normalized flow gradient structure). Theorem 21 gives a Lyapunov function but not a gradient flow. Row-normalizing  $v_i$  by  $Z_i$  introduces an asymmetry whenever  $Z_i \neq Z_j$ , so  $dG/dt$  has indefinite sign.

*Open Problem 5* (Full nonlinear ReLU clustering). Theorem 25 establishes the  $O(n \log d)$  vs.  $O(n)$  separation in the linearized regime under scalar-head equiangular assumptions. A full proof additionally requires handling (a) the non-smooth boundary  $\{\langle x_i, x_j \rangle = 0\}$ , where the ODE must be interpreted via Dini derivatives or regularization, and (b) the nonlinear regime  $\gamma = \Omega(1)$ , where a comparison argument with the full ODE (23) is needed.

## References

- [1] L. Ambrosio, N. Gigli, and G. Savaré. *Gradient Flows in Metric Spaces and in the Space of Probability Measures*. Birkhäuser, 2005.
- [2] J. L. Ba, J. R. Kiros, and G. E. Hinton. Layer normalization. arXiv:1607.06450, 2016.
- [3] G. Bruno, F. Pasqualotto, and A. Agazzi. Emergence of meta-stable clustering in mean-field transformers. In *ICLR*, 2025.
- [4] S. Chen, Z. Lin, Y. Polyanskiy, and P. Rigollet. Quantitative clustering in mean-field transformer models. arXiv:2504.14697, 2025.

- [5] S. Chen, Z. Lin, Y. Polyanskiy, and P. Rigollet. Critical attention scaling in long-context transformers. In *ICLR*, 2026.
- [6] Z. Chen, Y. Polyanskiy, and P. Rigollet. Clustering with Wasserstein–Fisher–Rao gradient flows. In *NeurIPS Workshop*, 2025.
- [7] C. Criscitiello, Q. Rebjock, A. D. McRae, and N. Boumal. Synchronization on circles and spheres with nonlinear interactions. arXiv:2405.18273, 2024.
- [8] B. Geshkovski, H. Koubbi, Y. Polyanskiy, and P. Rigollet. Dynamic metastability in the self-attention model. arXiv:2410.06833, 2024.
- [9] B. Geshkovski, C. Letrouit, Y. Polyanskiy, and P. Rigollet. The emergence of clusters in self-attention dynamics. In *NeurIPS*, 2023. arXiv:2305.05465.
- [10] B. Geshkovski, C. Letrouit, Y. Polyanskiy, and P. Rigollet. A mathematical perspective on transformers. *Bulletin of the American Mathematical Society*, 62(3):427–479, 2025. arXiv:2312.10794.
- [11] N. K. Jha and B. Reagen. Entropy-guided attention for private LLMs. arXiv:2501.03489, 2025.
- [12] N. Karagodin, S. Ge, Y. Polyanskiy, and P. Rigollet. Normalization in attention dynamics. In *NeurIPS*, 2025.
- [13] N. Karagodin, Y. Polyanskiy, and P. Rigollet. Clustering in causal attention masking. In *NeurIPS*, 2024.
- [14] Y. Kuramoto. Self-entrainment of a population of coupled non-linear oscillators. In *International Symposium on Mathematical Problems in Theoretical Physics*, 1975.
- [15] Y. Polyanskiy, P. Rigollet, and A. Yao. Synchronization of mean-field models on the circle. arXiv:2507.22857, 2025.
- [16] P. Rigollet. The mean-field dynamics of transformers. arXiv:2512.01868, 2025.
- [17] Z. Wang, Y. Shen, B. Yang, Y. Li, and C. Ding. A study on ReLU and softmax in transformer. arXiv:2302.06461, 2023.
- [18] A. Tomihari and R. Karakida. Recurrent self-attention dynamics: An energy-agnostic perspective from Jacobians. In *NeurIPS*, 2025.
- [19] A. Vaswani, N. Shazeer, N. Parmar, J. Uszkoreit, L. Jones, A. N. Gomez, Ł. Kaiser, and I. Polosukhin. Attention is all you need. In *NeurIPS*, 2017.
- [20] M. Wortsman, J. Lee, J. Gilmer, and S. Kornblith. Replacing softmax with ReLU in vision transformers. arXiv:2309.08586, 2023.
- [21] S. Zhai, T. Likhomanenko, E. Littwin, D. Busbridge, J. Ramapuram, Y. Zhang, J. Gu, and J. M. Susskind. Stabilizing transformer training by preventing attention entropy collapse. In *ICML*, 2023.